Numerical Analysis of a Floating Offshore Wind Turbine by Coupled Aero-hydrodynamic Simulation

Yang Huang, Ping Cheng and Decheng Wan*

Collaborative Innovation Center for Advanced Ship and Deep-Sea Exploration, State Key Laboratory of Ocean Engineering, School of Naval Architecture, Ocean and Civil Engineering, Shanghai Jiao Tong University, Shanghai 200240, China

Abstract: Due to environmental issues like global warming and energy crisis, the exploration for renewable and clean energies becomes crucial. In recent years, the floating offshore wind turbines (FOWTs) draw a great deal of attention as a means to exploit the steadier and stronger wind sources available in deep-sea areas. In the present study, the coupled aero-hydrodynamic characteristics of a spar-type 5-MW wind turbine are analyzed. An unsteady actuator line model (UALM) coupled with a two-phase CFD solver naoe-FOAM-SJTU is applied to solve the three-dimensional Reynolds-Averaged Navier-Stokes (RANS) equations. Simulations with different complexity are performed: firstly, the wind turbine is parked; secondly, the impact of wind turbine is simplified into equivalent forces and moments; thirdly, the fully coupled dynamic analysis with wind and wave excitation is conducted by utilizing the UALM. From the simulation, aerodynamic forces including the unsteady aerodynamic power and thrust can be obtained, and hydrodynamic responses such as the six-degree-of-freedom motions of the floating platform and the mooring tensions are also available. Based on simulations results, the coupled responses of the floating offshore wind turbine for cases of different complexity are analyzed. It is found that the coupling effects between the aerodynamics of wind turbine and the hydrodynamics of floating platform is obvious. The aerodynamic loads have significant effect on the dynamic responses of the floating platform, and the aerodynamic performance of the wind turbine presents highly unsteady characteristics due to the motions of the floating platform.

Keywords: floating offshore wind turbine; coupled aero-hydrodynamics; naoe-FOAM-SJTU solver; unsteady actuator line model; coupling effects

Article ID: 1671-9433(2016)01-0000-00

1 Introduction

The fossil fuels have always been the major source of energy for the last century. However, the traditional fossil energy is non-renewable energy sources and causes serious environmental pollution. Therefore, the exploration of renewable and clean energies is becoming crucial to the future of human being.

Wind energy is one of the most promising nonpolluting renewable energy sources, and it is also the fastest growing clean and renewable energy in recent years. A wind farm located offshore could experience average wind speeds 90% greater than a land-based wind farm (Archer and Jacobson, 2005), which means that the FOWTs have great potential to exploit the enormous offshore wind resources. On the other hand, wind farms in deep waters are in general less sensitive to space availability, noise restriction, visual pollution, and regulatory problems compared with onshore wind farms (Bae *et al.*, 2011). However, most of the wind farm development has been limited to land space or shallow water areas where depth does not exceed 50m. In recent years, some countries start to plan offshore floating wind farms. Considering the fact that the total cost of fixed-mounted offshore wind turbines increases with water depth, the FOWTs can provide the most cost effective and reasonable approach in deep sea areas (Butterfield *et al.*, 2005). And offshore floating wind farms are expected to produce huge amount of clean electricity at a competitive price compared to other energy sources.

Although the floating-type wind farms are more economical than the fixed ones in offshore areas where water depth is more than 40m (Henderson *et al.*, 2002; 2004; Musial *et al.*, 2004; Tong, 1998), there are many disadvantages of floating-type wind farms. For example, the complexity in blade controls due to the motion of floating platform, larger inertia loading on tall tower caused by greater floater accelerations and possible more expensive and complicated installation processes (Luo *et al.*, 2012). And compared with onshore wind turbines, the loads exposed on the FOWTs are more complex. Furthermore, considering the coupling effects between the wind turbine and the floating platform, integrated aero-hydrodynamic analysis for the FOWTs with wind and wave excitation is challenging.

It is known that aerodynamics analysis of FOWTs is significantly different from fixed wind turbines as it is shown to more unsteady resulted from effects of platform motions (Sebastian and Lackner, 2012). A computational fluid dynamics model for simulations of rotor under floating platform-induced motions was developed to study the unsteadiness and nonlinear aerodynamics in turbine operations (Wu and Nguyen, 2017). And computational fluid dynamics (CFD) approaches are used to study the aerodynamic performance of wind turbine coupled with the prescribed motions of floating platform. It is found that the

*Corresponding author Email: dcwan@sjtu.edu.cn

© Harbin Engineering University and Springer-Verlag Berlin Heidelberg 2016

unsteady aerodynamic thrust and power tend to vary considerably depending on the oscillation frequency and amplitude of the surge motion (Tran and Kim, 2016). The power coefficient and the instantaneous aerodynamic forces coefficients sensitively change with different pitching periods and pitching amplitudes (Lei *et al.*, 2017). And the flow interaction phenomena between the rotating wind turbine blades with oscillating motions and generated blade-tip vortices was observed (Tran and Kim, 2015). In addition, some scaled model tests were conducted to research the influence of the platform-induced motions on the power performances of the FOWTs. (Sant *et al.*, 2015; Hansen *et al.*, 2014; Ren *et al.*, 2014; Stewart *et al.*, 2012).

Understanding the coupling effects between the aerodynamics of wind turbine and the hydrodynamics of floating platform is beneficial to the design of FOWTs. The six-degree-of-freedom natural frequencies of the FOWTs are typically much lower than rotor-induced loadings (Roddier *et al.*, 2010; Nielsen *et al.*, 2006), so the possibility of dynamic resonance with that high-frequency excitations is of much less concern. However, the TLP-type FOWTs cannot ignore the dynamic resonance due to the high natural frequencies in the vertical-plane modes (Bae and Kim, 2010; Jagdale and Ma, 2010). Furthermore, the coupling effects between the wind turbine and the floating platform for a 5 MW TLP-type FOWT was studied (Matha, 2009). In additionally, some studies focusing on the coupled aero-hydrodynamics of the spar-type FOWTs are conducted. Two independent computer programs SIMO/RIFLEX and HAWC2 were combined to a coupled simulation tool for the simulation of the dynamic response of floating wind turbines exposed to forces form wind, wave and current (Nielsen *et al.*, 2006). Coupled wave and wind-induced motions of the catenary moored spar floating wind turbine under operational and extreme sea states was analyzed. Advanced blade element momentum theory was applied to study the aerodynamics. The DeepC code was used to calculate the displacement-force of mooring lines, and dynamic motion of the system due to the wave in harsh environmental conditions was considered in HAWC2 (Karimirad and Moan, 2012; Karimirad *et al.*, 2009). The effects of loads induced by wind and wave on a spar-type floating wind turbine were discussed. And the aerodynamic loads was calculated by FAST (Ma *et al.*, 2015). Based on a nonlinear computational model, the motion of a 5-MW spar type floating wind turbine in operational and extreme sea states with irregular waves was studied. Moreover, it was found that the higher aspect ratio spars generally lead to lower mean pitch and surge responses (Nematbakhsh *et al.*, 2014). It is fair to say that the research on integrated dynamic response for floating wind turbine is limited and further research is required (Karimirad and Moan, 2010).

In the present study, the coupled aero-hydrodynamic characteristics of a spar-type 5-MW wind turbine are analyzed. An unsteady actuator line model (Li *et al.* 2015) coupled with a two-phase CFD solver naoe-FOAM-SJTU is applied to solve the three-dimensional Reynolds-Averaged Navier-Stokes (RANS) equations. To research the coupling effects between the aerodynamics of wind turbine and the hydrodynamics of floating platform, simulations with different complexity are performed. From the simulation, aerodynamic forces including the unsteady aerodynamic power and thrust can be obtained, and hydrodynamic responses such as the six-degree-of-freedom motions of the floating platform and the mooring tensions are also available. Based on simulations results, the coupled responses of the floating offshore wind turbine for cases of different complexity are analyzed. Proper discussions on the fully coupled aero-hydrodynamics of the FOWT are presented.

2 Numerical Method

2.1 Unsteady Actuator Line Model

The actuator line model (ALM) that ignores the boundary layer of the blade and does not need complicated dynamic mesh is a simplified method to study the performance of the wind turbine, which can greatly reduce the quantity of grids and calculation time. The blade of wind turbine is simplified into actuator line in ALM, and the actuator lines withstanding body forces are divided into a series of discrete actuator units (Sørensen and Shen, 2002).

When the ALM is applied to the simulation of the FOWTs, the velocity vector ($\boldsymbol{U_M}$) induced by the motions of the floating platform is added into the velocity triangle (as Fig. 1 shows), which will lead to complex interactions between the rotor and its wake. So the ALM need to be modified to solve the unsteady problem caused by the dynamic motion responses of floating platform. The unsteady actuator line model considering the effect of six-degree-of-freedom motions is applied in this paper.

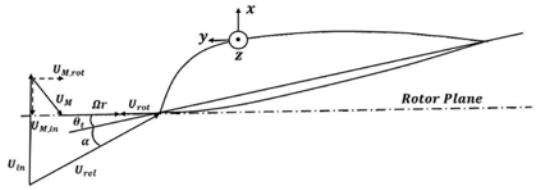

Fig. 1 Cross-sectional airfoil element

In order to determine the body forces acting on the rotor blades, a blade element method combined with two-dimensional airfoil characteristics is used. As Fig. 1 shows, a cross-sectional element at radius r defines the airfoil in the (x, y) plane. The integral velocity vector relationship is described as:

$$\boldsymbol{U_{rel}} = \boldsymbol{U_{in}} + (\Omega \times \boldsymbol{r}) + \boldsymbol{U_{rot}} + \boldsymbol{U_M} \quad (1)$$

The local velocity relative to the rotating blade is given as:

$$|U_{rel}| = \sqrt{(U_{in} - U_{M,in})^2 + (\Omega r - U_{rot} + U_{M,rot})^2} \quad (2)$$

The attack angle is defined as:

$$\alpha = \phi - \theta_t \quad (3)$$

Where $\phi = \tan^{-1}\left(\frac{U_{in}-U_{M,in}}{\Omega r - U_{rot}+U_{M,rot}}\right)$ is the inflow angle. θ_t is

the local twist angle. And the body force can be given by the following equation:

$$\boldsymbol{f} = (\boldsymbol{L},\boldsymbol{D}) = \frac{\rho|U_{rel}|^2 c N_b}{2rd\theta dz}(C_L\boldsymbol{e}_L + C_D\boldsymbol{e}_D) \quad (4)$$

Where c is the chord length; N_b is the number of blades; C_L and C_D are the lift and drag coefficient, respectively; $\boldsymbol{e}_L$ and $\boldsymbol{e}_D$ denote the unit vectors in the directions of the lift and the drag, respectively. The lift and drag coefficients are determined from measured or computed two-dimensional airfoil data that are corrected for three-dimensional effects.

The body force need to be smoothed to avoid singular behavior before it is added into the momentum equations.

$$\boldsymbol{f}_\varepsilon = \boldsymbol{f} \otimes \eta_\varepsilon \quad (5)$$

where

$$\eta_\varepsilon(d) = \frac{1}{\varepsilon^3\pi^{3/2}} exp\left[-\left(\frac{d_i}{\varepsilon}\right)^2\right] \quad (6)$$

Here d_i is the distance between the measured point and the initial force points on the rotor. ε is a constant that serves to adjust the strength of regularization function, and the influence of the parameter ε has been studied and some experienced conclusions have been obtained (Sørensen *et al*, 1998).

Then the body force can be written as:

$$\boldsymbol{f}_\varepsilon(x,y,z,t) = \sum_{i=1}^{N} \boldsymbol{f}_i(x_i,y_i,z_i,t) \frac{1}{\varepsilon^3\pi^{3/2}} exp\left[-\left(\frac{d_i}{\varepsilon}\right)^2\right] \quad (7)$$

And $\boldsymbol{f}_\varepsilon$ is the loading which is introduced as a body force on the right hand of the momentum equations.

2.2 Six-degree-of-freedom Motions

The solver naoe-FOAM-SJTU is able to predict the motion responses of the floating platform. Two coordinate systems (as shown in Fig. 2) are used in the procedure of solving six-degree-of-freedom motion equations. At each time step simulation, the motion equations are solved in platform-fixed coordinate system and the forces are calculated in earth-fixed coordinate system. The added velocity induced by the dynamic motions of the supporting platform is updated by the following equation:

$$\boldsymbol{U}_{motion,i} = [\boldsymbol{J}](\boldsymbol{U}_c + \boldsymbol{\omega}_c \cdot (x_i - x_c)) \quad (8)$$

Where $[\boldsymbol{J}]$ is the transformation matrix defined from the platform-fixed coordinate to earth-fixed coordinate; $\boldsymbol{U}_c$ and $\boldsymbol{\omega}_c$ donate the translation velocity and the angular velocity of the rotating center, respectively; x_c is the position coordinate of the rotating center.

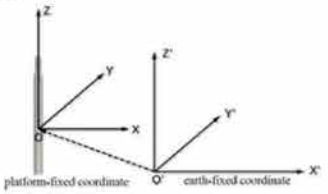

Fig. 2 Coordinate systems

2.3 Coupled Analysis Method

In the present work, the UALM is embedded into two-phase CFD solver naoe-FOAM-SJTU to study the coupled aero-hydrodynamic responses of the FOWTs. As Fig. 3 shows, the aerodynamic forces can be got by the UALM, and the six-degree-of-freedom motions are predicted by the naoe-FOAM-SJTU. Moreover, the piecewise extrapolating method (PEM) is used to research the performance of the mooring system.

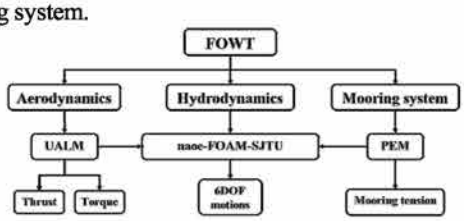

Fig. 3 Coupled analysis modules

The CFD solver naoe-FOAM-SJTU is developed by Professor Wan Decheng and his CFD team based on the open source tool packages OpenFOAM. VOF method with bounded compression technique is applied in the solver to solve two-phase flow problem with free surface. And the *k-ω* SST turbulence model is applied to solve the RANS equation due to the closure problem. The governing equations can be written as:

$$\nabla \cdot \boldsymbol{U} = 0 \quad (9)$$

$$\frac{\partial \rho \boldsymbol{U}}{\partial t} + \nabla \cdot (\rho(\boldsymbol{U} - \boldsymbol{U}_g))\boldsymbol{U} = -\nabla p_d - \boldsymbol{g} \cdot x\nabla\rho + \nabla \cdot (\mu_{eff}\nabla \boldsymbol{U}) + (\nabla \boldsymbol{U}) \cdot \nabla\mu_{eff} + \boldsymbol{f}_\sigma + \boldsymbol{f}_s + \boldsymbol{f}_\varepsilon \quad (10)$$

Where $\boldsymbol{U}$ is velocity of field; $\boldsymbol{U}_g$ is the velocity of mesh points; $p_d = p - \rho\boldsymbol{g} \cdot x$ is the dynamic pressure, subtracting hydrostatic component from total pressure; $\boldsymbol{g}$ is the gravity of acceleration vector; ρ is the mixture density with two phases; $\mu_{eff} = \rho(\nu + \nu_t)$ is effective dynamic viscosity, in which ν and ν_t are kinematic viscosity and eddy viscosity respectively; $\boldsymbol{f}_\sigma$ is the surface tension term in two phases model and takes effect only on the liquid free surface; $\boldsymbol{f}_s$ is the source term for sponge layer, which is set to avoid the wave reflection at the end of the tank and takes effect only in sponge layer; $\boldsymbol{f}_\varepsilon$ is the body force calculated from UALM, representing the effect of turbine blades on the flow field.

The solving procedure of coupled aero-hydrodynamic simulation for the FOWTs is shown in Fig. 4.

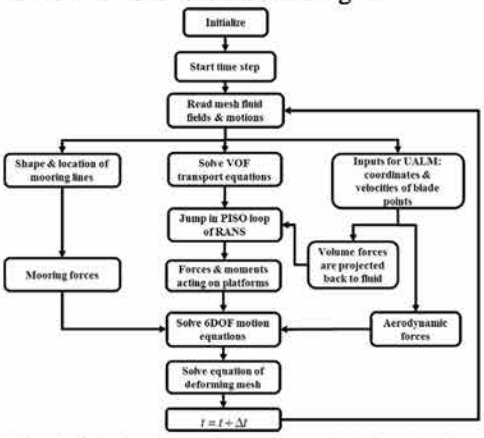

Fig. 4 Solving procedure of coupled simulation

3 Simulation Conditions

3.1 Geometric Model

Since the present work aims to study the coupled aero-hydrodynamic characteristics of the FOWTs, a spar-type 5-MW floating offshore wind turbine called OC3-Hywind turbine system is adopted. Figure 5 shows the sketch of the OC3-Hywind turbine system.

The wind turbine of OC3-Hywind turbine system is NERL offshore 5-MV baseline wind turbine, which is a conventional three-bladed, upwind, variable-speed and variable blade-pitch-to-feather controlled turbine. The main properties of the wind turbine are listed in Table 1 (Jonkman *et al.*, 2009).

Table 1 Specification of NERL 5-MW turbine

Rating	5 MW
Rotor Orientation, Configuration	Upwind, 3 Blades
Control	Variable Speed, Collective Pitch
Drivetrain	High Speed, Multiple-Stage Gearbox
Rotor, Hub Diameter	126 m, 3 m
Hub Height	90 m
Cut-in, Rated, Cut-out Wind Speed	3 m/s, 11.4 m/s, 25 m/s
Cut-in, Rated Rotor Speed	6.9 rpm, 12.1 rpm
Rated Tip Speed	80 m/s
Overhang, Shaft Tilt, Precone Angle	5 m, 5° ,2.5°
Rotor Mass	110,000 kg
Nacelle Mass	240,000 kg
Tower Mass	347,460 kg
Coordinate Location of Overall CM (center of mass)	(-0.2 m, 0.0 m, 64.0 m)

The floating platform of the FOWT is the spar-buoy concept platform called Hywind, and detailed information about the platform is give in Table 2 (Jonkman and Musial, 2010).

Table 2 Specification of Hywind platform

Depth to Platform Base Below SWL (Total Draft)	120 m
Elevation to Platform Top (Tower Base) Above SWL	10 m
Depth to Top of Taper Below SWL	4 m
Depth to Bottom of Taper Below SWL	12 m
Platform Diameter Above Taper	6.5 m
Platform Diameter Below Taper	9.4 m
Platform Mass, Including Ballast	7,466,330 kg
CML Location Below SWL Along Platform Center Line	89.9155 m
Platform Roll Inertia about CM	4,229,230,000 kg•m^2
Platform Pitch Inertia about CM	4,229,230,000 kg•m^2
Platform Yaw Inertia about Platform Centerline	164,230,000 kg•m^2

The mooring system consisting of threes mooring lines is symmetrically distributed around the platform. Main characteristics of the mooring system are shown in Table 3. And the arrangement of the mooring lines is shown in Fig. 6. The wind and the wave are in the same direction.

Table 3 Specification of the mooring system

Number of Mooring Lines	3
Angle Between Adjacent Lines	120°
Depth to Anchors Below SWL (water depth)	320 m
Depth to Fairleads Below SWL	70.0 m
Radius to Anchors Form Platform Centerline	853.87 m
Radius to Fairleads Form Platform Centerline	5.2 m
Unstretched Mooring line length	902.2 m
Mooring Line Diameter	0.09 m
Equivalent Mooring Line Mass Density	77.7066 kg/m
Equivalent Mooring Line Mass Weight in Water	689.094 N/m
Equivalent Mooring Line Extensional Stiffness	384,243,000 N
Additional Yaw Spring Stiffness	98,340,000 Nm/rad

Fig. 5 Sketch of the FOWT

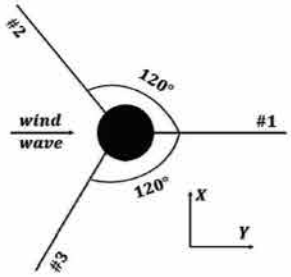

Fig. 6 Mooring system

3.2 Simulation Cases

To investigate the coupling effects between the wind turbine and the floating platform, simulations with different complexity are performed: firstly, the wind turbine is parked; secondly, the impact of wind turbine is simplified into equivalent forces and moments; thirdly, the fully coupled dynamic analysis with wind and wave excitation is conducted. Finally, three cases listed in Table 4 are selected in the present study. The wind speed in these case are kept in the same at a rated wind speed of U = 11.4m/s. The first order stokes wave is chosen as the incident wave in all simulation cases. The period of incident wave is T = 10s, and the wave length is about λ = 156m. The wave height is H = 4m.

Table 4 Simulation cases

	Simulation conditions descriptions
Case 1	Parked case: the wind turbine is parked
Case 2	Simplified case: the impact of wind turbine is simplified into equivalent forces and moments
Case 3	Coupled case: fully coupled aero-hydrodynamic simulation

3.3 Computation Domain and Grids

For case 1 and case 2, the aerodynamic performance of wind turbine is not the research focus. To reduce the quality of grids and save calculation time, the height of air phase is set to h_1 = 40m. The length and width of computation domain are 3 λ and 2 λ respectively. The depth of water phase is set to be 70% of the real water depth (d = 320m), for the effect of the water depth on the motion responses can be ignored at that water depth. The floating offshore wind turbine system is placed at the middle of the computation domain, 1 λ form the inlet boundary. And the length of sponge layer before outlet boundary is 100m. The computation domain for case 1 and case 2 is shown in Fig. 7(a). For case 3, fully coupled simulation for the FOWT is conducted. Considering the expansion effect of the turbine wake, the height of air phase is set to h_2 = 280m. The other arrangement of the computation domain for case 3 is just the same with case1 and case 2, which is shown in Fig. 7(b).

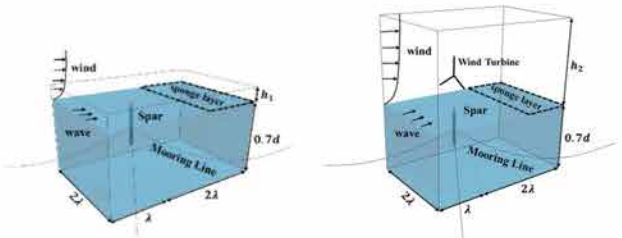

(a) Case 1 and Case 2 **(b) Case 3**

Fig.7 Computation domain

To capture the complex wake produced by the wind turbine, the refined grids are utilized in the region behind the wind turbine. And the grids near the water surface are refined to capture the free surface. The grid distribution is shown in Fig. 8.

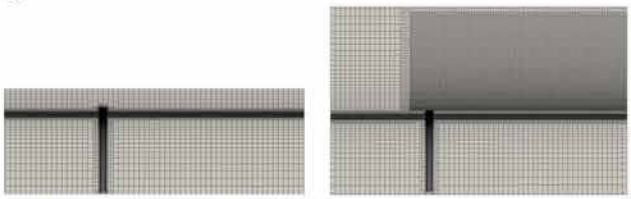

(a) Case 1 and Case 2 **(b) Case 3**

Fig. 8 Grid distribution

3.4 Boundary Conditions

The setup of boundary conditions in all simulation cases are the same, which are shown below:

(1) Inlet boundary: velocity condition is wave inlet condition, and pressure condition is Neumann boundary condition that the normal gradient of pressure is equal to zero;

(2) Outlet boundary: velocity condition is inletoutlet condition defined in OpenFOAM, and pressure condition is Dirichlet boundary condition that the pressure is constant;

(3) Top boundary: both velocity condition and pressure condition are Dirichlet boundary conditions;

(4) Bottom boundary: both velocity condition and pressure condition are slip conditions;

(5) Left boundary and right boundary: boundary conditions are defined as symmetry plane that directional derivative perpendicular to the boundary is equal to zero;

(6) Body surface: the moving wall boundary condition is adopted.

4 Results and Discussions

4.1 Aerodynamic Loads

Coupled aero-hydrodynamic simulation for the OC3-Hywind turbine system is conducted in the coupled case, and the aerodynamic loads including rotor torque and thrust are calculated by the UALM. The time history curves of the aerodynamic power and thrust are shown in Fig. 9 and Fig. 10 respectively.

It can be observed that the aerodynamic loads present obviously unsteady characteristics. The aerodynamic power and thrust both fluctuate greatly due to the dynamic motion responses of floating platform. And the aerodynamic loads change periodically, which means that the wind turbine suffers serious fatigue loading. The varying period is about 10s, which is approximately equal to the incident wave period. It indicates that the main cause for the periodical change of the aerodynamic loads is the pitch motion of floating platform, for the pitch motion is typical wave-frequency motion.

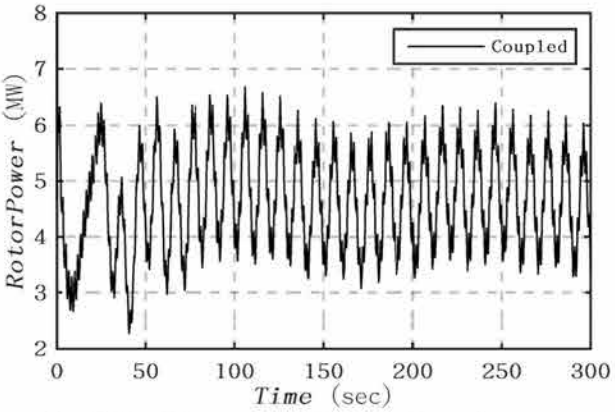

Fig. 9 Time history of transient aerodynamic power

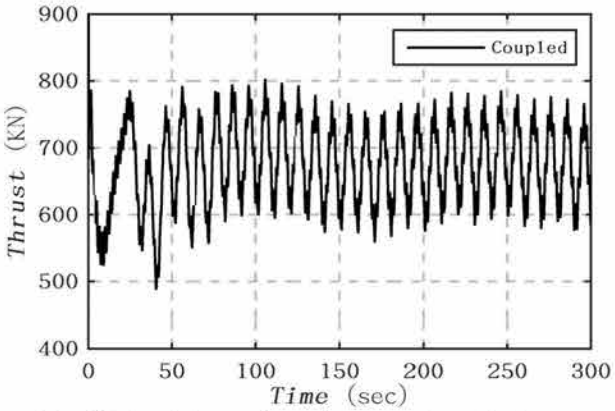

Fig. 10 Time history of transient aerodynamic thrust

Compared with the standard values of aerodynamic loads in the literature (Jonkman *et al.*, 2009), the average values of aerodynamic loads in coupled aero-hydrodynamic simulation are smaller, which is shown in Table 5. The aerodynamic power and thrust are decreased by 11% and 14% respectively. This means that the coupling effects between the wind turbine and the floating platform have a negative effect on the aerodynamic power output.

Table 5 Comparison of the aerodynamic power and thrust

	Standard value	Coupled case value	Decreased percentage
Power	5.3 MW	4.7 MW	11%
Thrust	787 KN	678 KN	14%

Considering the facts that the aerodynamic loads vary greatly due to the motions of floating platform and the aerodynamic power output decreases because of the coupling effects, proper control strategy should be taken to reduce the adverse effect of the motion responses on the aerodynamic performance of the FOWT.

4.2 Motion Responses

The floating platform is an important part of the FOWT, and the hydrodynamic performance of the platform has a significant effect on the aerodynamic power output and operation stability of the FOWT. To investigate the influence of the aerodynamic forces on the motion responses of the floating platform, simulations with different complexity are performed. For the parked case, the wind turbine is parked, so the influence of the aerodynamic forces can be ignored. For the simplified case, the aerodynamic forces are reduced to a constant thrust and a moment acting on the gravitational center of the platform, which is called simplified forces model. And the value of constant thrust is equal to the average value of thrust calculated in the coupled case. For the coupled case, fully coupled dynamic analysis with the wind and wave excitation is conducted, and the coupling effects between the wind turbine and the floating platform is considered.

The time history of six-degree-of-freedom motion responses of the floating platform under different simulation conditions are shown in Figs. 11(*a*)-11(*f*). The dash-dotted line represents the motion responses in the parked case, while the dotted line and the solid line correspond to the motion responses in the simplified case and the coupled case respectively.

Compared with the motion responses in the parked case that the effects of aerodynamic forces are ignored, it can be seen from Fig. 11 that the amplitude and fluctuation range of the motion responses in the simplified case and the coupled case are much larger. The reason is that the influence of aerodynamic forces on the motion responses is taken into account in the simplified case and the coupled case. It can be found that the aerodynamic forces derived from the wind turbine have remarkable impact on the motion responses of the platform. Especially in surge, pitch and yaw motion responses, the effect of aerodynamic forces is more significant. In the simplified case and the coupled case, the predicted maximum value of surge motion exceeds 20m and the predicted mean value of pitch motion is about 4 degrees, which leads to strong interaction between the rotor and its wake. Furthermore, it indicates that the motion responses of floating platform will result in the unsteady aerodynamic performance of the FOWT.

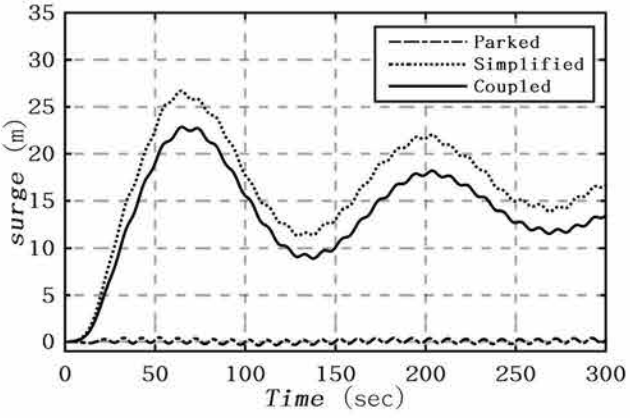

(*a*) Surge

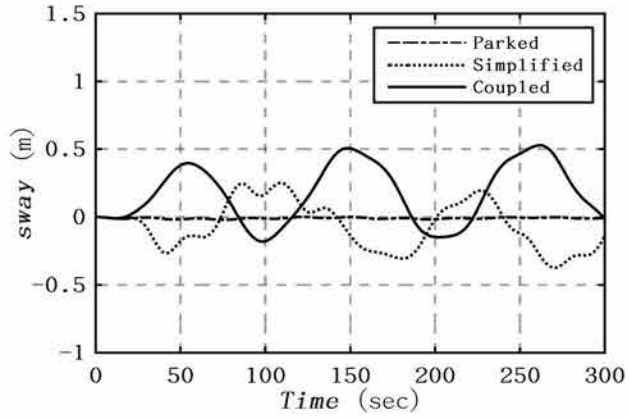

(*b*) Sway

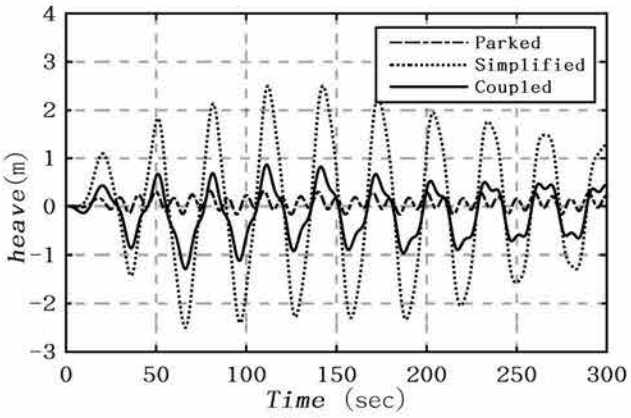

(*c*) Heave

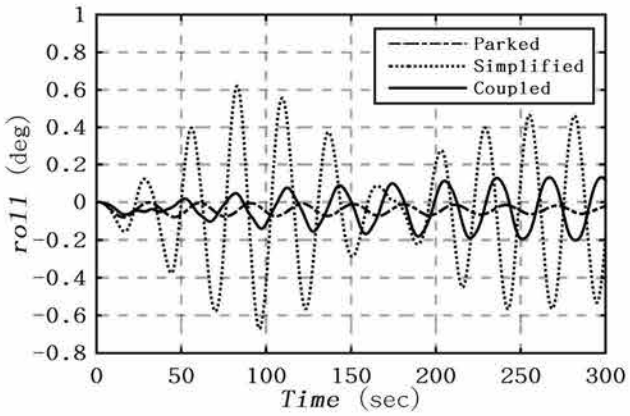

(*d*) Roll

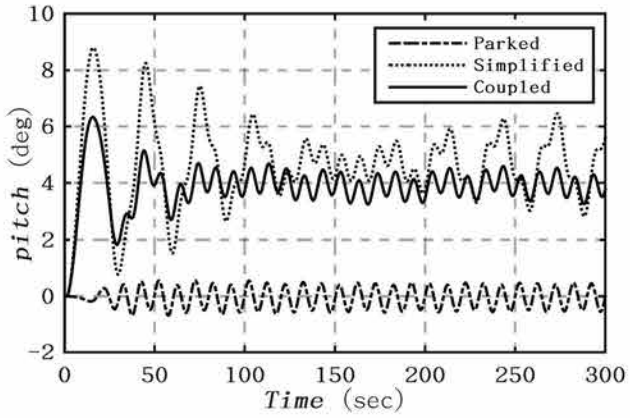

(*e*) Pitch

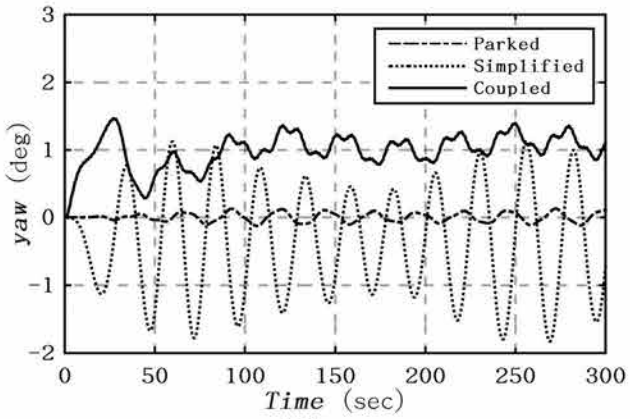

(*f*) Yaw

Fig. 11 Comparison results of the platform motion responses

In the simplified case, as the dotted line shown in Fig. 11, the motion responses of the platform are over-predicted compared with those in the coupled case. It can be seen that the maximum surge motion in the simplified case is 4m larger than that in the coupled case. And the mean value of pitch motion in the simplified case is slightly bigger than that in the coupled case. Moreover, the amplitude of yaw motion in the simplified case is much larger than that in the coupled case, while the mean value of yaw motion in the simplified case is smaller than that in the coupled case. Although the influence of aerodynamic forces on the motion responses is taken into consideration in the simplified case, the coupling effects between the aerodynamics of wind turbine and the hydrodynamics of floating platform are ignored. This result in the motion responses have great discrepancy in the simplified case and the coupled case. Furthermore, it indicates that the coupling effects have significant effect on the motion responses, and the simplified force model regarding the aerodynamic forces as a constant thrust and a moment leads to the over-prediction of motion responses.

In summary, the motion responses of the FOWT under wind and wave excitation is dominated by the aerodynamic forces instead of the wave loads. And the coupling effects between the aerodynamics of wind turbine and the hydrodynamics of floating platform have a great influence on the motion responses of the FOWT, so fully coupled aero-hydrodynamic simulation is necessary for the study of motion responses of the FOWT.

4.3 Mooring System Responses

The comparison results of the time history of mooring tensions under different simulation conditions are shown in Figs. 12(*a*)-12(*c*).

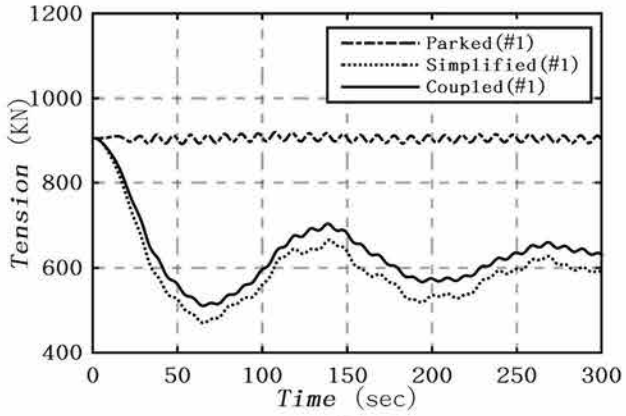

(*a*) Line #1

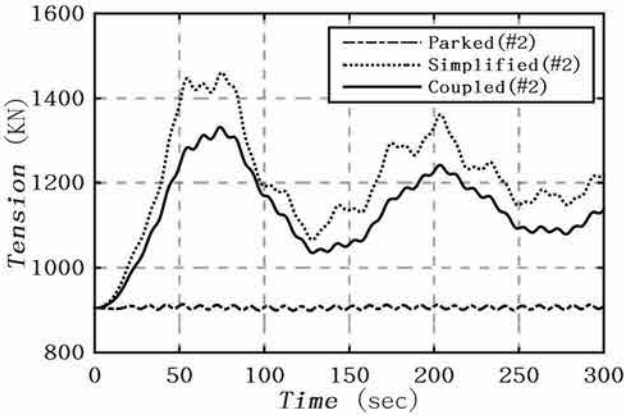

(*b*) Line #2

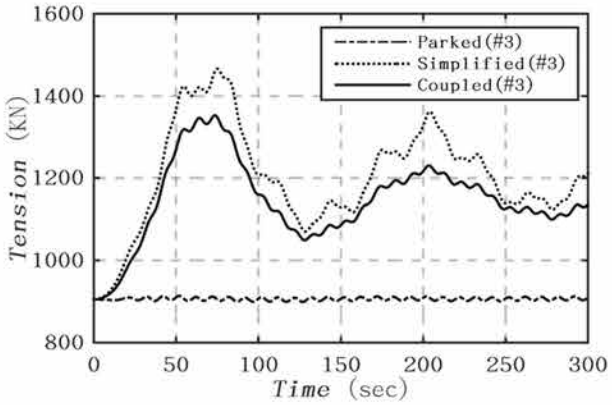

(*c*) Line #3

Fig. 12 The time history of mooring tensions

Compared with Fig. 11(*a*), it can be seen from Figs. 12(*a*)-12(*c*) that the trend of the mooring tension is similar to the surge motion of floating platform, which suggests that the tensions of mooring lines mainly depend on the amplitude of surge motion. Additionally, contrasting Fig. 12(*b*) with Fig. 12(*c*), it can be found that the tension of mooring line #3 is almost identical to that of mooring line #2 resulting from the mooring line #3 is placed symmetric to mooring line #2 along wave direction. The slightly difference between the tension of mooring line #2 and that of mooring line #3 is due to the yaw motion of floating platform.

Herein, the comparison results of the tension of mooring line #1 are analyzed to study the performance of mooring system under different simulation conditions. It can be seen from Fig. 12(*a*) that the mooring tension in the parked case is much smaller than that in the simplified case and the coupled case. And the mooring tension in the simplified case is obviously larger than that in the coupled case. As analyzed above, the surge motions under different simulation conditions result in this discrepancy among the mooring tensions. The larger the amplitude of surge motion is, the larger the mooring tension will be. Considering the significant influence of aerodynamic forces on the motion responses, the fluctuating range of the mooring tension is great due to the large drift displacement of the platform. So the risk of failure for mooring lines should be noted.

4.4 Wake Vortex

The wake vortex has a significant influence on the aerodynamic characteristics of wind turbine. The evolution of wake vortex at different times of an entire wave circle is illustrated in Figs. 13(*a*)-13(*d*). The wave is contoured by wave height and the mooring lines are represented by three black lines. The second-order invariant of velocity gradient tensor, Q (Digraskar, 2010), is used to visualize the wake vortex. And the Q is calculated by the following equation:

$$Q_{ij} = \frac{1}{2}(\Omega_{ij} \times \Omega_{ij} - S_{ij} \times S_{ij}) \quad (11)$$

Where Ω_{ij} and S_{ij} donate the strength of the vortex and the shear strain rate respectively.

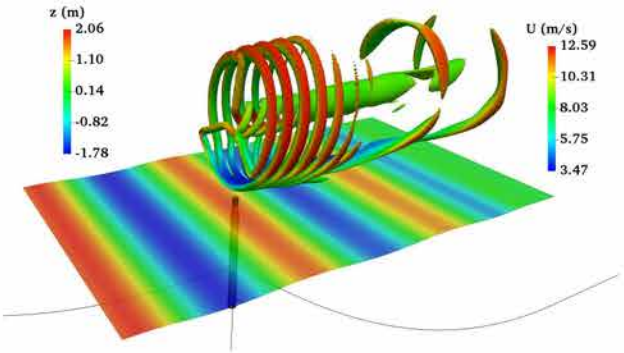

(*a*) Time = 0 *T*

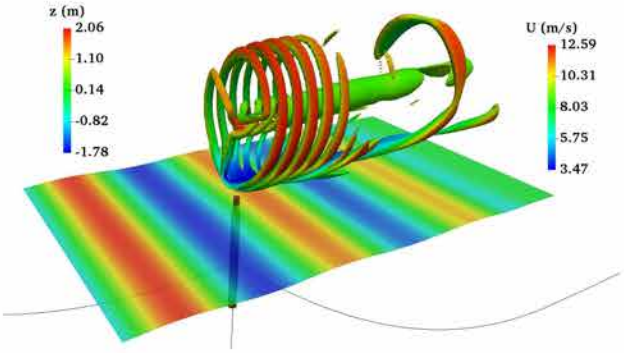

(*b*) Time = 0.25 *T*

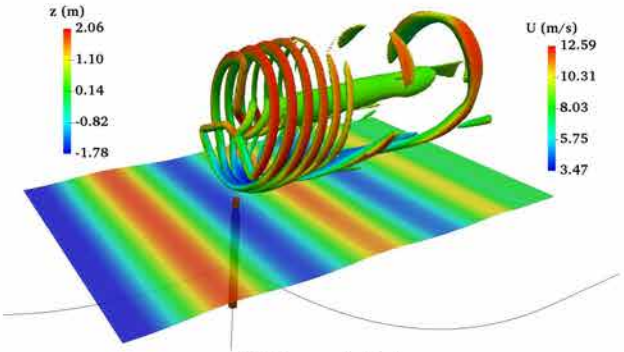

(*c*) Time = 0.5 *T*

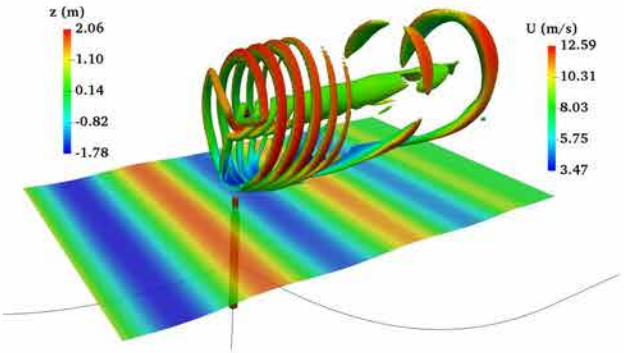

(*d*) Time = 0.75 *T*

Fig.13 Instantaneous vortex structure of the rotor

From Figs. 13(*a*)-13(*d*), it can be clearly seen that the spiral tip vortex generated in the wake is captured. However, this vorticity is quickly diffused in the downstream. And the tip vortex expands and fragments with time. It can also be found that the vortex structure in the wake leans backward obviously, resulting from the motions of floating platform. It suggests that the wake vortex is highly unsteady in coupled aero-hydrodynamic simulation of the FOWT considering the coupling effects between the wind turbine and the floating platform.

5 Conclusions

In this paper, the unsteady actuator line model is embedded into two-phase CFD solver naoe-FOAM-SJTU to achieve coupled aero-hydrodynamic simulation of OC3-Hywind turbine system. Simulations with different complexity are performed: firstly, the wind turbine is parked; secondly, the impact of wind turbine is simplified into equivalent forces and moments; thirdly, the fully coupled dynamic analysis with wind and wave excitation is conducted. Based on the simulation results, fully coupled dynamic responses of the floating offshore wind turbine including the aerodynamic loads, wake vortex, motion responses, and mooring tensions are compared and analyzed to study the coupling effects between the aerodynamics of wind turbine and the hydrodynamics of floating platform. It has been found that the aerodynamic loads present periodical change due to the motion responses of floating platform. And the moving platform has a negative effect on the aerodynamic power output. Compared with the standard value of the aerodynamic loads, the aerodynamic power and thrust decrease by 11% and 14% respectively. Furthermore, the motion responses of floating platform are found to be dominated by the aerodynamic forces derived from the wind turbine instead of the wave loads. And the coupling effects have significant influence on the motion responses. Fully coupled aero-hydrodynamic simulation is necessary for the study of dynamic motion responses of the FOWT. For the mooring system, large fluctuation of the mooring tension is observed due to the large drift displacement of the platform. So the risk of failure for mooring lines should be noted. Moreover, it can be seen from the wake vortex structure that the motion responses of floating platform result in strong interaction between the rotor and its wake, which increases the instability of the aerodynamic performance. So proper control strategy should be taken to reduce the adverse effect of the motion responses on the aerodynamic performance of the FOWT. In order to improve the understanding of coupling effects and provide more accurate numerical model for practical application, more coupled aero-hydrodynamic simulations for the FOWT under different wind and wave conditions should be performed in the near future.

6 Acknowledgements

This work is supported by the National Natural Science Foundation of China (51379125, 51490675, 11432009, 51579145), Chang Jiang Scholars Program (T2014099), Shanghai Excellent Academic Leaders Program (17XD1402300), Shanghai Key Laboratory of Marine Engineering (K2015-11), Program for Professor of Special Appointment (Eastern Scholar) at Shanghai Institutions of Higher Learning (2013022), Innovative Special Project of Numerical Tank of Ministry of Industry and Information Technology of China(2016-23/09) and Lloyd's Register Foundation for doctoral student, to which the authors are most grateful.

References

Archer CL, Jacobson MZ, 2005. Evaluation of global wind power. *Journal of Geophysical Research*, 110 (D12): 12110. DOI: 10.1029/2004JD005462.

Bae, YH, Kim MH, Yu Q, Kim K, 2011. Influence of control strategy to FOWT hull motions by aero-elastic-control-floater-Mooring coupled dynamic analysis. *International Offshore & Polar Engineering Conference*. International Society of Offshore and Polar Engineers.

Bae YH, Kim MH, Shin YS, 2010. Rotor-floater-mooring coupled dynamic analysis of mini TLP-type offshore floating wind Turbines. *the 29th International Conference on Ocean, Offshore and Arctic Engineering*, 3:491-498. DOI: 10.1115/OMAE2010-20555.

Butterfield S, Musial W, Jonkman J, Prof Paul Sclavounos, 2005. Engineering challenges for floating offshore wind turbines. *Copenhagen Offshore Wind 2005 Conference and Expedition Proceedings*, 13(1): 25-28.

Digraskar DA, 2010. *Simulations of flow over wind turbines*. Master thesis, University of Massachusetts Amherst.

Hansen AM, Laugesen R, Bredmose H, Mikkelsen R, Psichogios N, 2014. Small scale experimental study of the dynamic response of a tension leg platform wind turbine. *Journal of Renewable and Sustainable Energy*, 6(5): 033104-465. DOI: 10.1063/1.4896602.

Henderson AR, Zaaijer MB, Bulder B, Pierik J, Huijsmans R, Van Hees M, Snijders E, Wijnants GH, Wolf MJ, 2004. Floating windfarms for shallow offshore sites. *Proceedings of the Fourteenth International Offshore and Polar Engineering Conference*, Toulon, France, May 23-28.

Henderson AR, Leutz R, Fujii T, 2002. Potential for floating offshore wind energy in Japanese waters. *Proceedings of the Twelfth International Offshore and Polar Engineering Conference*, Kitakyushu, Japan, May 26-31.

Jagdale S, Ma QW, 2010. Practical simulation on motions of a TLP-type support structure for offshore wind turbines. *Proceedings of the Twentieth International Offshore and Polar Engineering Conference*, Beijing, China, June 20-25.

Jonkman J, Musial W, 2010. Offshore code comparison collaboration (OC3) for IEA task 23 offshore wind technology and deployment. *Office of Scientific & Technical Information Technical Reports*. DOI: NREL/TP-5000-48191.

Jonkman J, Butterfield S, Musial W, Scott G, 2009. Definition of a 5-MW Reference wind turbine for offshore system

development. *Office of Scientific & Technical Information Technical Reports*.
DOI:10.1002/ajmg.10175.

Karimirad M, Moan T, 2010. Extreme structural dynamic response of a spar type wind turbine. *AMSE 2010, International Conference on Ocean, Offshore and Arctic Engineering*, 2010: 303–12.
DOI: 10.1115/OMAE2010-20044.

Karimirad M, Gao Z, Moan T, 2009. Dynamic motion analysis of catenary moored spar wind turbine in extreme environmental condition. *European Offshore Wind Conference 2009, Sweden*.

Karimirad M, Moan T, 2012. Wave-and wind-Induced dynamic response of a spar-type offshore wind turbine. *Journal of Waterway Port Coastal and Ocean Engineering*, 138 (1): 9–20.
DOI: 10.1061/(ASCE)WW.1943-5460.

Lei H, Zhou D, Lu J, Chen C, Han Z, Bao Y, 2017. The impact of pitch motion of a platform on the aerodynamic performance of a floating vertical axis wind turbine. *Energy*, 119: 369–383.
DOI:10.1016/j.energy.2016.12.086.

Li PF, Cheng P, Wan DC, 2015. Numerical simulations of wake flows of floating offshore wind turbines by unsteady actuator line model. *Proceedings of the 9th International Workshop on Ship and Marine Hydrodynamics*, Glasgow, UK, 26 - 28 August.

Luo N, Garcés JLP, Seguí YV, Zapateiro M, 2012. Dynamic load mitigation for floating offshore wind turbines supported by structures with mooring lines. *àrees temàtiques de la upc::energies::energia eòlica*.

Ma Y, Hu Z, Xiao L, 2015. Wind-wave induced dynamic response analysis for motions and mooring loads of a spar-type offshore floating wind turbine. *Journal of Hydrodynamics*, 26 (6): 865–74.
DOI:10.1016/S1001-6058(14)60095-0.

Matha D, Fischer T, Kuhn M, 2009. Model development and loads analysis of an offshore wind turbine on a tension leg platform. *the 2009 European Offshore Wind Conference and Exhibition*, Stockholm, Sweden, September 14-16.

Musial W, Butterfield S, Boone A, 2004. Feasibility of floating platform systems for wind turbines. *the 23rd ASME Wind Energy Symposium*, Reno, Nevada, January 5-8.
DOI: 10.2514/6.2004-1007.

Nematbakhsh, A, Olinger DJ, Tryggvason G, 2014. Nonlinear simulation of a spar buoy floating wind turbine under extreme ocean conditions. *Journal of Renewable and Sustainable Energy*, 6 (3): 708-720.
DOI: 10.1063/1.4880217.

Nielsen FG, Hanson TD, Skaare B, 2006. Integrated dynamic analysis of floating offshore wind turbines. *American Society of Mechanical Engineers*, 1: 671–679.
DOI: 10.1115/omae2006-92291

Ren, N, Li Y, Ou J, 2014. Coupled wind-wave time domain analysis of floating offshore wind turbine based on computational fluid dynamics method. *Journal of Renewable and Sustainable Energy*, 6(2): 53-86.
DOI: 10.1063/1.4870988.

Roddier D, Cermelli C, Aubault A, Weinstein A, 2010. WindFloat: A floating foundation for offshore wind turbines. *Journal of Renewable and Sustainable Energy*, 2 (3):53.
DOI: 10.1063/1.3435339.

Sant T, Bonnici D, Farrugia R, Micallef D, 2015. Measurements and modelling of the power performance of a model floating wind turbine under controlled conditions. *Wind Energy*, 18(5):811-834.
DOI: 10.1002/we.1730

Sebastian T, and Lackner MA, 2012. Characterization of the unsteady aerodynamics of offshore floating wind turbines. *Wind Energy*, 16(3):339-352.
DOI: 10.1002/we.545

Sørensen JN, Shen WZ, 2002. Numerical modeling of wind turbine wakes. *Journal of Fluid Engineering*, 124: 393–99.
DOI: 10.1115/1.1471361.

Sørensen JN, Shen WZ, Munduate X, 1998. Analysis of wake states by a full-field actuator disc model. *Wind Energy*, 1 (2): 73–88.
DOI:10.1002/(SICI)1099-1824(199812)1:2<73::AID-WE12>3.0.CO;2-L.

Stewart G, Lackner M, Robertson A, Jonkamn J, Goupee A, 2012. Calibration and validation of a FAST floating wind turbine model of the DeepCwind scaled tension-leg platform. *Proceedings for the 22th International Offshore and Polar Engineering Conference*, Rhodes, Greece, June 17-22.

Tong KC, 1998. Technical and economic aspects of a floating offshore wind farm. *Journal of Wind Engineering and Industrial Aerodynamics*, s 74–76(98): 399–410.
DOI: 10.1016/S0167-6105(98)00036-1.

Tran TT, Dong HK, 2015. The aerodynamic interference effects of a floating offshore wind turbine experiencing platform pitching and yawing motions. *Indian Journal of Thoracic and Cardiovascular Surgery*, 29 (2): 549–561.
DOI: 10.1007/s12206-015-0115-0.

Tran TT, Kim DH, 2016. A CFD study into the influence of unsteady aerodynamic interference on wind turbine surge motion. *Renewable Energy*, 90: 204–228.
DOI: 10.1016/j.renene.2015.12.013.

Wu CK, Nguyen V. 2017. Aerodynamic simulations of offshore floating wind turbine in platform-induced pitching motion. *Wind Energy*, 20 (5): 835–858.
DOI: 10.1002/we.2066.